Random uncertainties modelling for vibroacoustic frequency response functions of cars

J.-F. Durand, L. Gagliardini, Christian Soize

Random uncertainties modelling for vibroacoustic frequency response functions of cars

J.F. Durand[(1),(2)], **L. Gagliardini**[(1)], **C. Soize**[(2)]
[(1)] PSA Peugeot-Citroën
Route de Gisy - 78943 Vélizy-Villacoublay, France,

[(2)] Labratoire de Mécanique, Université de Marne-la-Vallée,
5, bd Descartes - 77454 Marne-la-Valée Cedex

email: **jeanfrancois.durand2@mpsa.com, jfdurand@univ-mlv.fr**

Abstract

This paper deals with the numerical prediction of the vibroacoustic frequency response functions of cars. In such a complex vibroacoustic system, the role played by data errors and model errors is important and does not have the same consequences for stiff structural element or for flexible (soft) structural element. A non-parametric probabilistic model of random uncertainties is introduced to study the sensitivity of these vibroacoustic frequency response functions. The method is applied to a simplified car body with an internal acoustic cavity. The confidence region of each random vibroacoustic frequency response function is numerically constructed. The results obtained, clearly show an important difference between the level of uncertainties for stiff and flexible structural elements.

1 Introduction

The design of cars is nowadays mainly based on the numerical simulations. In the case of vibroacoustics (for instance, for the booming noise), the problem of the predictability of the models are much more difficult due to the over-sensitiveness of the dynamical responses induced by structural complexity as much as uncertainties resulting from the industrial process. This over-sensitiveness is seen as well numerically (sensitiveness to modelling uncertainties) as in experiments (dispersion of the cars / process). Concerning the role played by uncertainties in structural dynamic modelling, it is known that the effects increase with the frequency. Consequently, in linear structural dynamics, numerical predictions with finite element models can be improved by introducing a model of random uncertainties. Random uncertainties in linear structural dynamics are usually modelled using probabilistic parametric models. Such an approach is difficult, even impossible, for taking into account the random uncertainties of a complex structure such as a car, within an industrial framework. Recently, a new approach that we call a non-parametric approach has been introduced for modelling random uncertainties in linear and non-linear elastodynamics for the low-frequency range, using the entropy optimization principle. This approach allows the direct construction of a probabilistic model of a reduced matrix model of the structure to be constructed. Such a non-parametric model does not require identifying the uncertain parameters as usually done for parametric approach. In the present case, the non-parametric method is applied to a structural-acoustic system in the low-frequency range, composed by the car body and the internal cavity. This paper is limited to study sensitivity of the vibroacoustic frequency response functions to random uncertainties in the stiffness operator of the structure (car body). The confidence region of the random vibroacoustic frequency response functions are numerically constructed which allows the sensitivity of stiff and flexible structural elements to uncertainties to be studied.

2 Statement of the structural-acoustics problem in the frequency domain

2.1 Geometry and mechanical assumptions

The physical space $\mathbb{R}^3$ is referred to a cartesian reference system and we denote the generic point of $\mathbb{R}^3$ as $\mathbf{x} = (x_1, x_2, x_3)$. We study the linear vibration of a structural-acoustic master system around a static equilibrium state taken as natural state at rest. The master system is defined as a master structure coupled with an internal acoustic cavity (see Figure 1).

2.1.1 Master structure Ω_S

The master structure at equilibrium occupies a three-dimensional bounded domain Ω_S of $\mathbb{R}^3$ with a sufficiently smooth boundary $\partial\Omega_S = \Gamma$. The outward unit normal to $\partial\Omega_S$ is denoted as $\mathbf{n}_S = (n_{S,1}, n_{S,2}, n_{S,3})$. The displacement field in Ω_S is denoted as $\mathbf{u}(\mathbf{x}, \omega) = (u_1(\mathbf{x}, \omega), u_2(\mathbf{x}, \omega), u_3(\mathbf{x}, \omega))$. The master structure is assumed to be free, i.e. not fixed on any part of boundary $\partial\Omega_S$.

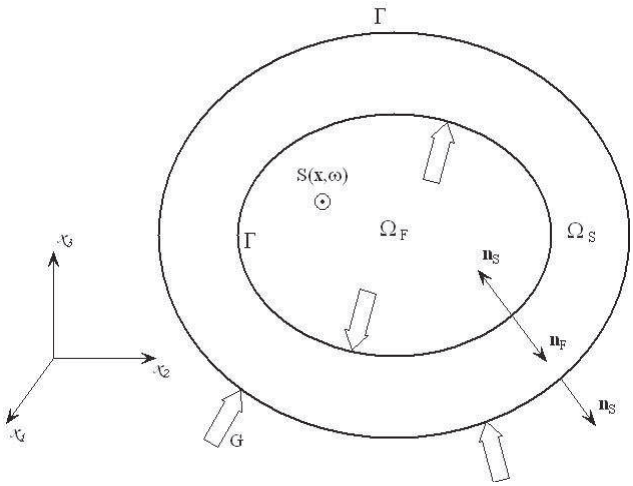

Figure 1: Configuration of the structural-acoustic master system

2.1.2 Internal acoustic cavity Ω_F

The internal acoustic cavity Ω_F is the bounded domain filled with a dissipative acoustic fluid. The boundary $\partial\Omega_F$ of Ω_F is Γ. The outward unit normal to $\partial\Omega_F$ is denoted as $\mathbf{n}_F = (n_{F,1}, n_{F,2}, n_{F,3})$ and we have $\mathbf{n}_F = -\mathbf{n}_S$ on $\partial\Omega_F$. We denote the pressure field in Ω_F as $p(\mathbf{x}, \omega)$.

2.2 Boundary value problem of the structural-acoustic master system

The equation of the master structure occupying domain Ω_S is written [1, 2, 3] as

$$-\omega^2 \rho_S u_i - \sigma_{ij,j} = g_i^{vol} \quad \text{in} \quad \Omega_S \quad , \tag{1}$$

in which ρ_S is the mass density, σ_{ij} is the stress tensor, $\mathbf{u} = (u_1, u_2, u_3)$ is the displacement field of the structure and $\mathbf{g}^{vol} = (g_1^{vol}, g_2^{vol}, g_3^{vol})$ is the body force field. The boundary condition can be written as

$$\sigma_{ij}(\mathbf{u}) n_{S,j} = g_i^{surf} - p\, n_{S,i} \quad \text{on} \quad \Gamma \quad . \tag{2}$$

in which $\mathbf{g}^{surf} = (g_1^{surf}, g_2^{surf}, g_3^{surf})$ is the surface force field, and p is the fluid pressure field at the coupling interface. The material is assumed to be linear viscoelastic without memory which allows the constitutive equation to be defined.
Concerning the internal acoustic fluid, a formulation in terms of pressure $p(\mathbf{x}, \omega)$ is used. The equation governing the dynamics of the acoustic fluid is written [4, 5, 6, 7] as

$$\frac{\omega^2}{\rho_F c_F^2} p + i\omega \frac{\tau}{\rho_F} \nabla^2 p + \frac{1}{\rho_F} \nabla^2 p = \frac{\tau}{\rho_F} c_F^2 \nabla^2 s - i \frac{\omega}{\rho_F} s \quad \text{in} \quad \Omega_F \,, \tag{3}$$

$$\frac{1}{\rho_F}(1 + i\omega\tau) \frac{\partial p}{\partial \mathbf{n}_F} = \omega^2 \mathbf{u}.\mathbf{n}_F + \tau \frac{c_F^2}{\rho_F} \frac{\partial s}{\partial \mathbf{n}_F} \quad \text{on} \quad \Gamma \quad . \tag{4}$$

where ρ_F is the mass density of the fluid, c_F is the speed of sound , τ represents the coefficient due to the viscosity of the fluid, and $s(\mathbf{x}, \omega)$ is the source term.

2.3 Finite element discretization

The finite element method [8] is used. We consider a finite element mesh of the master structure Ω_S and of the internal fluid Ω_F. The two meshes are assumed to be compatible on the coupling interface Γ. Let $\underline{\mathbf{u}}^S = (\underline{u}_1^S, \ldots, \underline{u}_{n_S}^S)$ be the complex vector of the n_S degrees of freedom (DOF) of the structure corresponding to the finite element discretization of the displacement field $\mathbf{u}$. Let $\underline{\mathbf{p}}^F = (\underline{p}_1^F, \ldots, \underline{p}_{n_F}^F)$ be the complex vector of the n_F DOF of the fluid corresponding to the finite element discretization of the pressure field p. Therefore, the finite element discretization of the boundary value problem in terms of $\mathbf{u}$ and p [4, 7, 9], defined by Eqs. (1) to (4) yields the following matrix equation

$$\begin{bmatrix} [\underline{A}^S(\omega)] & [\underline{C}] \\ \omega^2 [\underline{C}]^T & [\underline{A}^F(\omega)] \end{bmatrix} \begin{bmatrix} \underline{\mathbf{u}}^S(\omega) \\ \underline{\mathbf{p}}^F(\omega) \end{bmatrix} = \begin{bmatrix} \underline{\mathbf{f}}^S(\omega) \\ \underline{\mathbf{s}}^F(\omega) \end{bmatrix} \tag{5}$$

where $[\underline{A}^S(\omega)]$ is the dynamical stiffness matrix of the structure which is a symmetric $(n_S \times n_S)$ complex matrix such that

$$[\underline{A}^S(\omega)] = -\omega^2 [\underline{M}_{n_S}^S] + i\omega [\underline{D}_{n_S}^S] + [\underline{K}_{n_S}^S] \quad ,$$

in which $[\underline{M}_{n_S}^S]$, $[\underline{D}_{n_S}^S]$, $[\underline{K}_{n_S}^S]$ are the mass, damping and stiffness matrices of the structure *in vacuo*. Matrix $[\underline{M}_{n_S}^S]$ is a positive-definite symmetric $(n_S \times n_S)$ real matrix, $[\underline{D}_{n_S}^S]$ and $[\underline{K}_{n_S}^S]$ are semipositive-definite symmetric $(n_S \times n_S)$ real matrices. In Eq. (5), $[\underline{A}^F(\omega)]$ is the dynamical stiffness matrix of the acoustic fluid which is a symmetric $(n_F \times n_F)$ complex matrix such that

$$[\underline{A}^F(\omega)] = -\omega^2 [\underline{M}_{n_F}^F] + i\omega [\underline{D}_{n_F}^F] + [\underline{K}_{n_F}^F] \quad ,$$

in which $[\underline{M}_{n_F}^F]$, $[\underline{D}_{n_F}^F]$, $[\underline{K}_{n_F}^F]$ are the mass, damping and stiffness matrices of the cavity with fixed coupling interface. Matrix $[\underline{M}_{n_F}^F]$ is a positive-definite symmetric $(n_F \times n_F)$ real matrix, $[\underline{D}_{n_F}^F]$ and $[\underline{K}_{n_F}^F]$ are semipositive-definite symmetric $(n_F \times n_F)$ real matrices.

Introducing the change of variable $\underline{\mathbf{p}}^F = i\omega \underline{\widetilde{\mathbf{p}}}^F$, Eq. (5) can be rewritten as the following symmetric matrix equation,

$$\begin{bmatrix} [\underline{A}^S(\omega)] & i\omega [\underline{C}] \\ i\omega [\underline{C}]^T & -[\underline{A}^F(\omega)] \end{bmatrix} \begin{bmatrix} \underline{\mathbf{u}}^S(\omega) \\ \underline{\widetilde{\mathbf{p}}}^F(\omega) \end{bmatrix} = \begin{bmatrix} \underline{\mathbf{f}}^S(\omega) \\ -\frac{1}{i\omega} \underline{\mathbf{s}}^F(\omega) \end{bmatrix} \tag{6}$$

2.4 Mean reduced matrix model of the structural-acoustic master system

The structural modes *in vacuo* and the acoustic modes of the cavity with fixed coupling interface are calculated by solving the two generalized eigenvalue problems,

$$[\underline{K}^S_{n_S}]\underline{\psi} = \underline{\lambda}^S[\underline{M}^S_{n_S}]\underline{\psi} \quad , \tag{7}$$

$$[\underline{K}^F_{n_F}]\underline{\phi} = \underline{\lambda}^F[\underline{M}^F_{n_F}]\underline{\phi} \quad . \tag{8}$$

The eigenvectors verify the usual orthogonal properties [10, 11, 12, 13]. The structure *in vacuo* has six rigid body modes corresponding to a zero eigenvalue and n structural modes (elastic modes). Since we are only interested in the elastic deformation of the structure, the structural displacement is written as

$$\underline{\mathbf{u}}^S(\omega) = [\underline{\Psi}]\,\underline{\mathbf{q}}^S(\omega) \quad , \tag{9}$$

in which $[\underline{\Psi}]$ is the $(n_S \times n)$ real matrix whose columns are constituted of the n structural modes associated with the n first positive eigenvalues (the n first structural eigenfrequencies). The internal acoustic cavity has one constant pressure mode and $m-1$ acoustic modes. The internal acoustic pressure is written as

$$\underline{\mathbf{p}}^F(\omega) = [\underline{\Phi}]\,\underline{\mathbf{q}}^F(\omega) \quad , \tag{10}$$

in which $[\underline{\Phi}]$ is the $(n_F \times m)$ real matrix whose columns are constituted (1) of the constant pressure mode associated with zero eigenvalue and (2) of the acoustic modes associated with the positive eigenvalues (the $m-1$ first acoustical eigenfrequencies). It should be noted that the constant pressure mode is kept in order to model the quasi-static variation of the internal fluid pressure induced by the deformation of the coupling interface [4]. Using Eqs. (9) and (10), the projection of Eq. (6) yields the mean reduced matrix model of the structural-acoustic master system,

$$\begin{bmatrix} [\underline{\mathcal{A}}^S(\omega)] & i\omega[\underline{\mathcal{C}}] \\ i\omega[\underline{\mathcal{C}}]^T & -[\underline{\mathcal{A}}^F(\omega)] \end{bmatrix} \begin{bmatrix} \underline{\mathbf{q}}^S(\omega) \\ \underline{\tilde{\mathbf{q}}}^F(\omega) \end{bmatrix} = \begin{bmatrix} \underline{\mathcal{F}}^S(\omega) \\ -\frac{1}{i\omega}\underline{\mathcal{S}}^F(\omega) \end{bmatrix} \tag{11}$$

in which

$$[\underline{\mathcal{A}}^S(\omega)] = [\underline{\Psi}]^T[\underline{A}^S(\omega)][\underline{\Psi}] \quad , \quad [\underline{\mathcal{A}}^F(\omega)] = [\underline{\Phi}]^T[\underline{A}^F(\omega)][\underline{\Phi}] \quad ,$$
$$[\underline{\mathcal{C}}] = [\underline{\Psi}]^T[\underline{C}][\underline{\Phi}] \quad , \quad [\underline{\mathcal{F}}^S(\omega)] = [\underline{\Psi}]^T[\underline{\mathbf{f}}^S(\omega)] \quad , \quad [\underline{\mathcal{S}}^F(\omega)] = [\underline{\Phi}]^T[\underline{\mathbf{s}}^F(\omega)] \quad .$$

The generalized dynamical stiffness matrix $[\underline{\mathcal{A}}^S(\omega)]$ of the structure is then written as

$$[\underline{\mathcal{A}}^S(\omega)] = -\omega^2[\underline{\mathcal{M}}^S] + i\omega[\underline{\mathcal{D}}^S] + [\underline{\mathcal{K}}^S] \quad , \tag{12}$$

in which, the positive-definite diagonal $(n \times n)$ real matrices $[\underline{\mathcal{M}}^S]$, $[\underline{\mathcal{D}}^S]$ and $[\underline{\mathcal{K}}^S]$ are such that $[\underline{\mathcal{M}}^S] = [\underline{\Psi}]^T[\underline{M}^S_{n^S}][\underline{\Psi}]$, $[\underline{\mathcal{D}}^S] = [\underline{\Psi}]^T[\underline{D}^S_{n^S}][\underline{\Psi}]$ and where

$$[\underline{\mathcal{K}}^S] = [\underline{\Psi}]^T[\underline{K}^S_{n^S}][\underline{\Psi}] \quad . \tag{13}$$

3 Non-parametric probabilistic model of random uncertainties

As explained in Section 1, this paper is limited to study structural stiffness uncertainties. These uncertainties are induced by data errors and by model errors. Due to the presence of model errors, the usual parametric probabilistic approach which is perfectly adapted for modelling data errors, cannot be used for modelling model errors. Consequently, we proposed to use a non-parametric probabilistic model of random uncertainties allowing data errors and model errors to be taken into account. Such a non-parametric probabilistic has been proposed in Refs. [14, 15, 16] and is used below.

Let $\mathbb{M}_n^+(\mathbb{R})$, be the set of all the positive-definite symmetric $(n \times n)$ real matrices. Since $[\underline{\mathcal{K}}^S]$ defined by Eq. (13) belongs to $\mathbb{M}_n^+(\mathbb{R})$, it can written that

$$[\underline{\mathcal{K}}^S] = [\underline{L}_n]^T [\underline{L}_n] \tag{14}$$

in which $[\underline{L}_n]$ is the positive-definite diagonal $(n \times n)$ real matrix whose diagonal terms are the square roots of the diagonal terms of $[\underline{\mathcal{K}}^S]$.

The non-parametric probabilistic approach of the structural stiffness uncertainties consists in substituting the generalized stiffness diagonal matrix $[\underline{\mathcal{K}}^S]$ by the full $(n \times n)$ random matrix $[\mathbf{K}_n]$ which is a $\mathbb{M}_n^+(\mathbb{R})$-valued random variable written as

$$[\mathbf{K}_n] = [\underline{L}_n]^T [\mathbf{G}_n] [\underline{L}_n] \quad . \tag{15}$$

In Eq. (15), $[\mathbf{G}_n]$ is a random matrix with values in $\mathbb{M}_n^+(\mathbb{R})$ whose mean value is the identity matrix and whose probability distribution on the set $\mathbb{M}_n^+(\mathbb{R})$ is explicitly constructed [14, 15]. The following algebraic representation of this random matrix $[\mathbf{G}_n]$ allows realizations to be easily constructed,

$$[\mathbf{G}_n] = [\mathbf{L}_n]^T [\mathbf{L}_n] \quad ,$$

in which $[\mathbf{L}_n]$ is a random upper triangular $(n \times n)$ real matrix whose random elements are independent random variables defined as follows:
(1) for $j < j'$, the real-valued random variable $[\mathbf{L}_n]_{jj'}$ is written as $[\mathbf{L}_n]_{jj'} = \sigma_n U_{jj'}$ in which $\sigma_n = \delta\,(n+1)^{-1/2}$ and where $U_{jj'}$ is a real-valued Gaussian random variable with zero mean and variance equal to 1;
(2) for $j = j'$, the positive-valued random variable $[\mathbf{L}_n]_{jj'}$ is written as $[\mathbf{L}_n]_{jj'} = \sigma_n \sqrt{2V_j}$ in which σ_n is defined above and where V_j is a positive-valued gamma random variable whose probability density function p_{V_j} with respect to dv is written as

$$p_{V_j}(v) = \mathbf{1}_{\mathbb{R}^+}(v)\, \frac{1}{\Gamma(\frac{n+1}{2\delta^2} + \frac{1-j}{2})}\, v^{(\frac{n+1}{2\delta^2} - \frac{1-j}{2})} e^{-v} \quad .$$

Consequently, the mean generalized structural dynamical stiffness matrix $[\underline{\mathcal{A}}^S(\omega)]$ defined by Eq. (12) becomes a random symmetric $(n \times n)$ complex matrix $[\mathbf{A}_n^S(\omega)]$ defined by

$$[\mathbf{A}_n^S(\omega)] = -\omega^2 [\underline{\mathcal{M}}^S] + i\omega [\underline{\mathcal{D}}^S] + [\mathbf{K}_n] \quad , \tag{16}$$

in which $[\mathbf{K}_n]$ is the $\mathbb{M}_n^+(\mathbb{R})$-valued random matrix defined by Eq. (15). With such a non-parametric probabilistic model, Eq. (11) is replaced by the following random matrix equation,

$$\begin{bmatrix} [\mathbf{A}_n^S(\omega)] & i\omega[\underline{\mathcal{C}}] \\ i\omega[\underline{\mathcal{C}}]^T & -[\underline{\mathcal{A}}^F(\omega)] \end{bmatrix} \begin{bmatrix} \mathbf{Q}^S(\omega) \\ \widetilde{\mathbf{Q}}^F(\omega) \end{bmatrix} = \begin{bmatrix} \underline{\mathcal{F}}^S(\omega) \\ -\frac{1}{i\omega}\underline{\mathcal{S}}^F(\omega) \end{bmatrix} \tag{17}$$

in which random matrix $[\mathbf{A}_n^S(\omega)]$ is defined by Eq. (16) and where, for fixed ω, $\mathbf{Q}^S(\omega)$ and $\widetilde{\mathbf{Q}}^F(\omega)$ are complex random vectors. For every ω, the random linear Eq. (17) is solved by using the Monte-Carlo numerical simulation. The random nodal displacement vector $\mathbf{U}^S(\omega)$ of the structure and the random nodal pressure vector $\mathbf{P}^S(\omega)$ of the acoustic fluid are calculated by

$$\mathbf{U}^S(\omega) = [\underline{\Psi}]\, \mathbf{Q}^S(\omega) \quad , \quad \mathbf{P}^F(\omega) = i\omega [\underline{\Phi}]\, \widetilde{\mathbf{Q}}^F(\omega) \quad . \tag{18}$$

3.1 Confidence region of the random vibroacoustic frequency response functions

Let $\omega \mapsto W(\omega) : B \to \mathbb{R}^+$ be the modulus of an observed vibroacoustic frequency response function (either the modulus of the frequency response function in displacement at a given point in the structure or the modulus of the frequency response function in pressure at a given point in the internal acoustic cavity). The confidence region associated with the probability level P_c for the random function $\{W(\omega), \omega \in B\}$ is constructed by using the quantiles. For fixed ω in B, let $F_{W(\omega)}$ be the cumulative distribution function (continuous from the right) of random variable $W(\omega)$ which is such that $F_{W(\omega)}(w) = P(W(\omega) \leq w)$. For $0 < p < 1$, the p-th quantile or fractile of $F_{W(\omega)}$ is defined as

$$\zeta(p) = \inf\{w : F_{W(\omega)}(w) \geq p\} \quad .$$

Then the upper envelope $w^+(\omega)$ and the lower envelope $w^-(\omega)$ of the confidence region are defined by

$$w^+(\omega) = \zeta(1 - P_c) \qquad , \qquad w^-(\omega) = \zeta(P_c) \quad .$$

The estimation of $w^+(\omega)$ and $w^-(\omega)$ is performed by using the sample quantiles [17]. Let $w_1(\omega) = W(\omega; \theta_1), \ldots, w_{n_r}(\omega) = W(\omega; \theta_{n_r})$ be the n_r independent realizations of random variable $W(\omega)$. Let $\widetilde{w}_1(\omega) < \ldots < \widetilde{w}_{n_r}(\omega)$ be the order statistics associated with $w_1(\omega), \ldots, w_{n_r}(\omega)$. Therefore, if fix($z$) is the integer part of the real number z, one has the following estimation

$$w^+(\omega) \simeq \widetilde{w}_{j^+}(\omega)\,,\; j^+ = \text{fix}(n_r(1 - P_c)) \quad , \quad w^-(\omega) \simeq \widetilde{w}_{j^-}(\omega)\,,\; j^- = \text{fix}(n_r(P_c)) \quad .$$

4 Vibroacoustics of a simplified car

4.1 Mean model of the structural-acoustic master system

The mean model is constituted of a simplified car body and an internal acoustic cavity. We are interested in studying the frequency response functions in the low-frequency band $B = [40, 200]Hz$, for given external loads induced by the engine. The finite element model of the structure has 14562 DOF corresponding to 3906 solid finite elements (see Figure 2). The internal acoustic cavity contains the seats. The finite element model of the internal acoustic cavity has 3347 DOF corresponding to 14150 acoustic fluid finite elements (see Figure 3). It should be noted that the two meshes are compatible on the fluid-structure coupling interface.

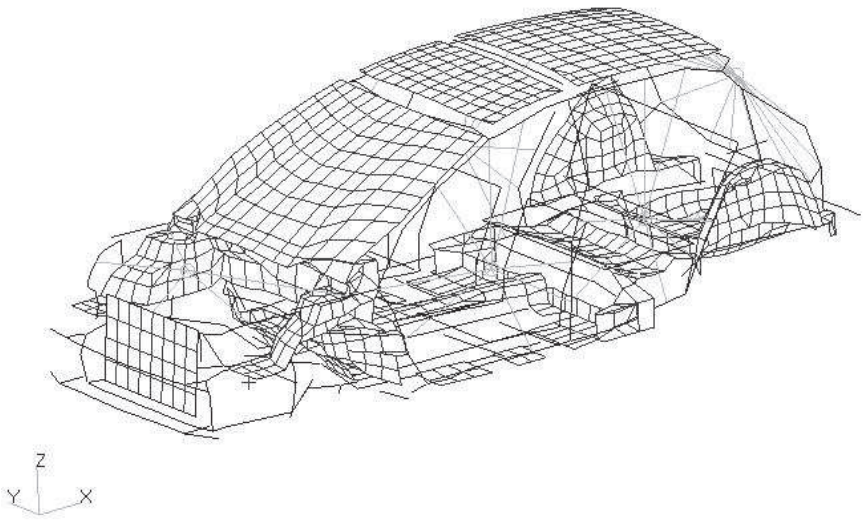

Figure 2: Finite element model of the structure

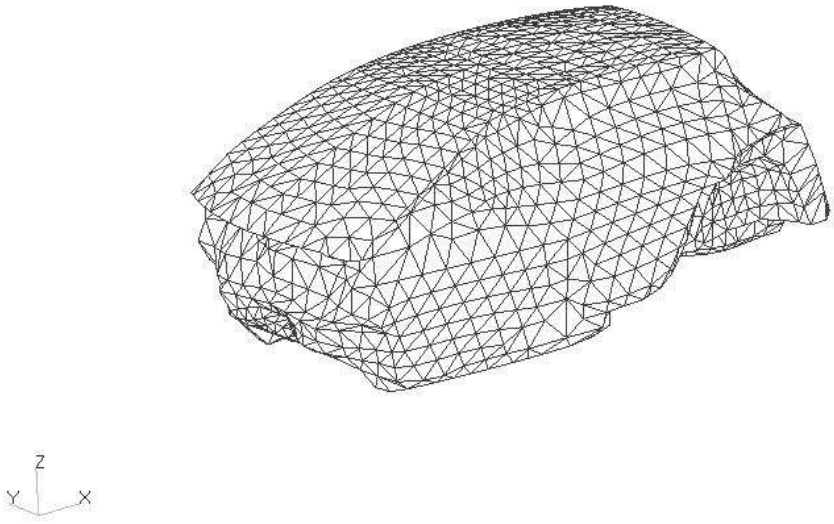

Figure 3: Finite element model of the internal acoustic cavity

4.2 Random vibroacoustic frequency responses of the structural-acoustic master system with random uncertainties

The random Eq. (17) is solved by using the Monte Carlo numerical simulation performed with a number of realizations n_r. The random displacement field of the structure and the random pressure field inside the internal acoustic cavity are then computed by using Eq. (18).

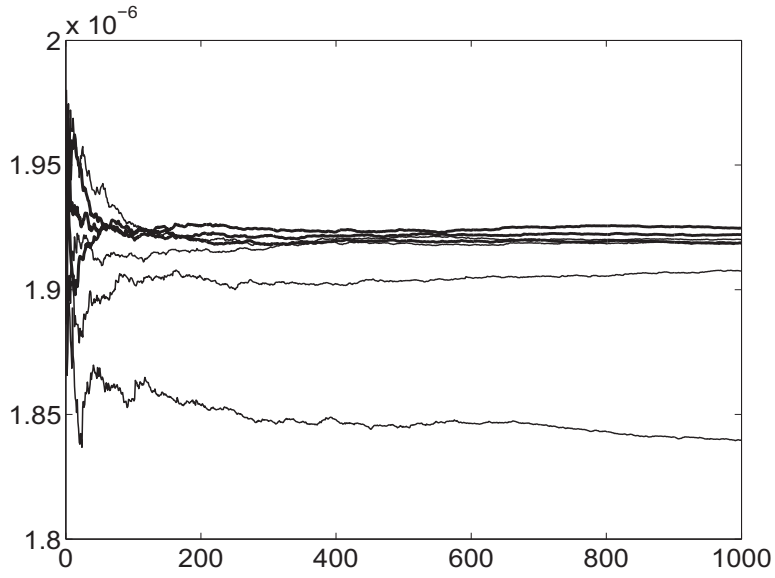

Figure 4: Graph of function $n_r \mapsto \text{conv}^S(n_r)$ related to the convergence of the random structural generalized coordinates. Horizontal axis: n_r, Vertical axis: $\text{conv}^S(n_r)$. Four lower thin solid lines are for (n, m)= (90,5), (n, m)= (137,10), (n, m)= (230,24), (n, m)= (269,35), three upper thick solid lines are for (n, m)= (303,51), (n, m)= (342,68), (n, m)= (380,51)

In this numerical application, the value of the dispersion parameter δ controlling the uncertainties of the stiffness matrix of the structure is such that δ=0.08.
The convergence of the random solution is analyzed in studying the graph of the function $n_r \mapsto \text{conv}^H(n_r)$

defined by

$$\text{conv}^H(n_r) = \frac{1}{n_r}\sum_{\ell=1}^{n_r}\int_B ||\mathbf{Q}^H(\omega;\theta_\ell)||^2 d\omega$$

in which exponent H is either S for the structure or F for the fluid and where $\mathbf{Q}^H(\omega;\theta_1),\ldots,\mathbf{Q}^H(\omega;\theta_{n_r})$ are the n_r realizations of the vector-valued random variable $\mathbf{Q}^H(\omega)$. Figure 4 displays the graph of the function $n_r \to \text{conv}^S(n_r)$ for the structure. Figure 5 displays the graph of the function $n_r \mapsto \text{conv}^F(n_r)$ for the internal acoustic cavity.

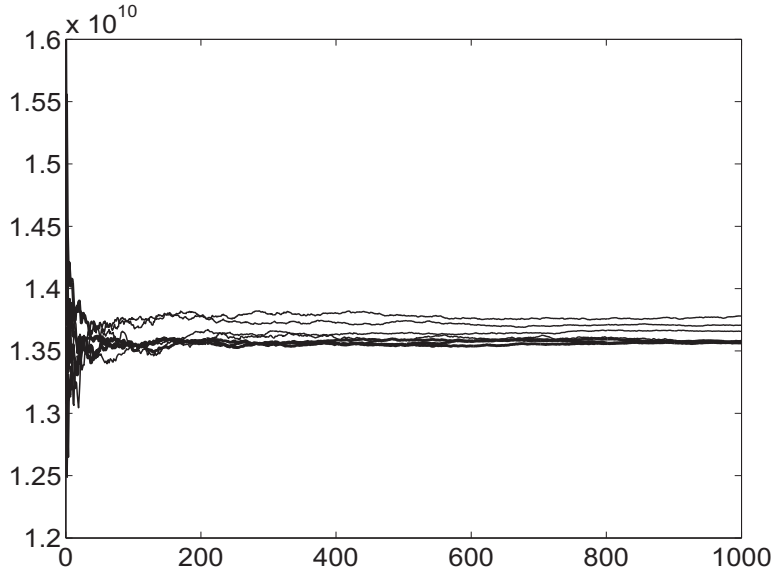

Figure 5: Graph of function $n_r \mapsto \text{conv}^F(n_r)$ related to the convergence of the random acoustic generalized coordinates. Horizontal axis: n_r, Vertical axis: $\text{conv}^F(n_r)$. Four upper thin solid lines are for (n,m)= (90,5), (n,m)= (137,10), (n,m)= (230,24), (n,m)= (269,35), three lower thick solid lines are for (n,m)=(303,51), (n,m)= (342,68), (n,m)= (380,51)

From these two figures (see Figures 4 and 5), it can be deduced that a reasonable mean-square convergence of the random structural-acoustic system is reached for $n_r = 600$ realizations, $n = 350$ structural modes and $m = 50$ acoustic modes. The confidence region of each random vibroacoustic frequency response function is constructed with the following values of the parameters: number of realizations for the Monte Carlo numerical simulation $n_r = 700$, number of structural modes $n = 350$, number of acoustic modes $m = 50$.

Figures 6 to 11 are relative to the confidence region prediction of the random frequency response functions. On each figure, the horizontal axis is the frequency axis in Hertz, the vertical axis is (1) $20\log 10(W(\omega))$ for structural displacements, (2) $20\log 10(W(\omega)/P_{ref})$ for internal acoustic pressures, (3) $10\log 10(W(\omega))$ for energies. The thick solid line is the graph of the response of the mean model, the thick dashed line is the mean value of the random frequency response and the grey region is the confidence region for a probability level $P_c = 0.95$.

Figure 6 displays the structural frequency response function for the structural normal displacement at a point located on the car roof. This is a flexible (soft) structural element. It can be seen a large confidence region for frequencies greater than 60 Hz. It can be concluded that such a soft structural element is sensitive to random uncertainties.

Figures 7 and 8 display the structural frequency response function for the structural z- and y-displacements at a point located in a stiff structural element. It can be seen a narrow confidence region for all the frequency band. It can be concluded that such a stiff structural element is less sensitive to random uncertainties.

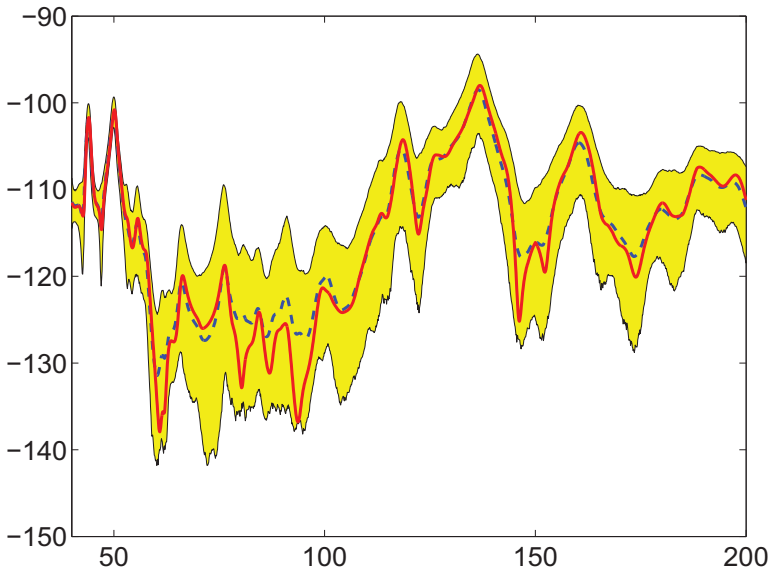

Figure 6: Confidence region of the random frequency response function for the structural normal displacement at a point located on the car roof: mean model prediction (thick solid line), mean response of the stochastic model (thick dashed line), confidence region (grey region)

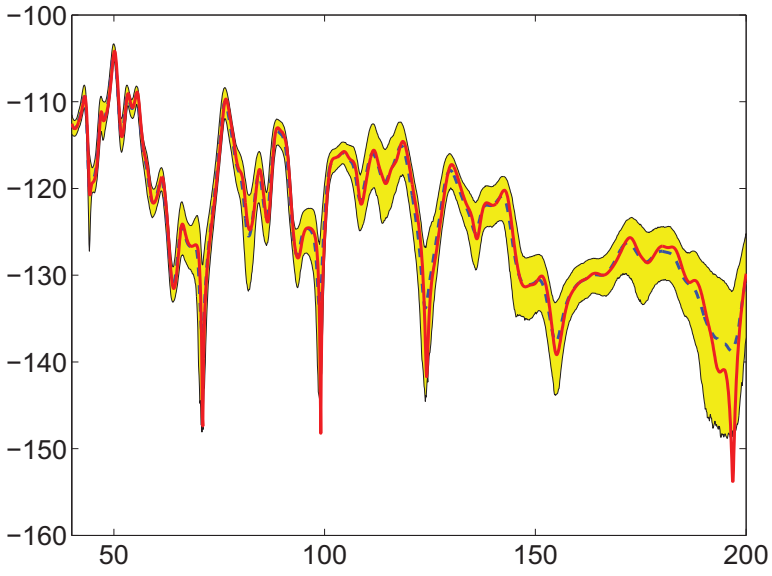

Figure 7: Confidence region of the random frequency response function for the structural z-displacement at a point located in a stiff structural element: mean model prediction (thick solid line), mean response of the stochastic model (thick dashed line), confidence region (grey region)

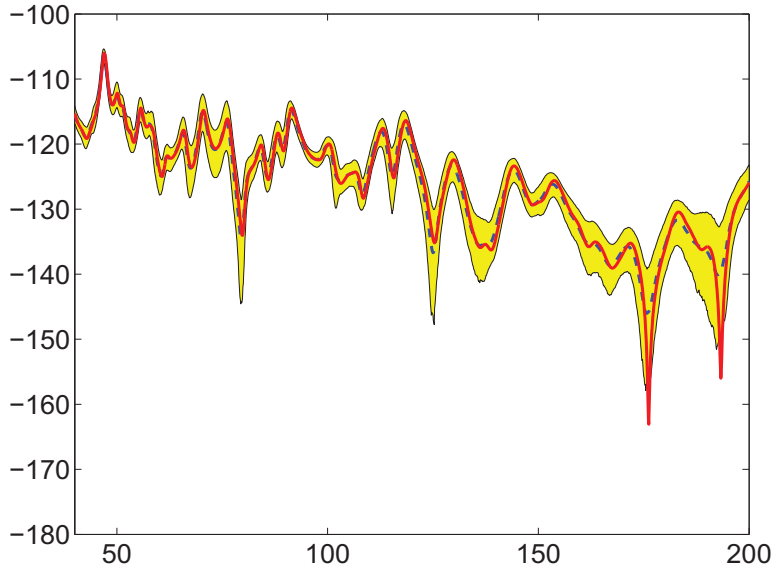

Figure 8: Confidence region of the random frequency response function for the structural y-displacement at a point located in a stiff structural element: mean model prediction (thick solid line), mean response of the stochastic model (thick dashed line), confidence region (grey region)

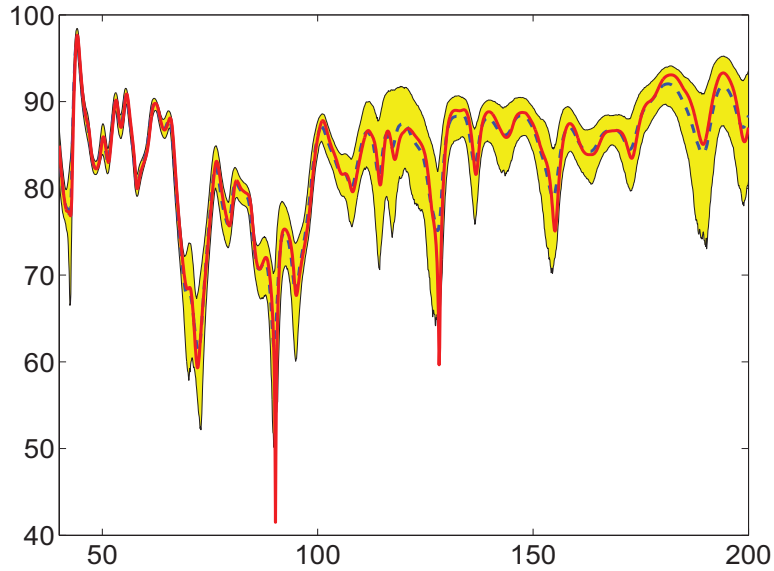

Figure 9: Confidence region of the random frequency response function for the internal acoustic pressure at a point located at the right passenger ear: mean model prediction (thick solid line), mean response of the stochastic model (thick dashed line), confidence region (grey region)

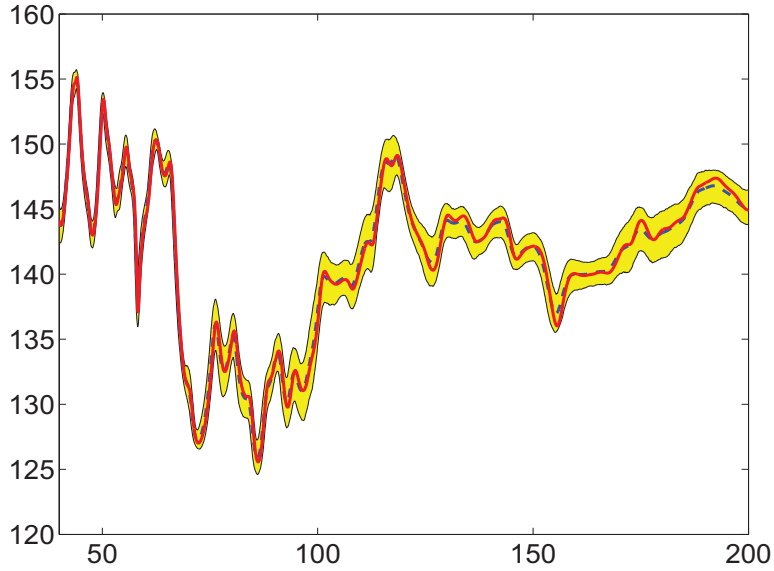

Figure 10: Confidence region of the random frequency response function for the total acoustic energy of the internal cavity: mean model prediction (thick solid line), mean response of the stochastic model (thick dashed line), confidence region (grey region)

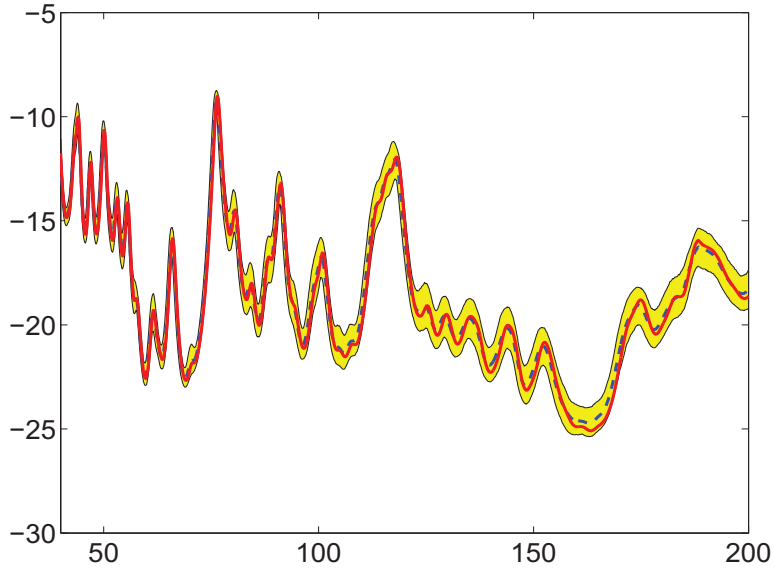

Figure 11: Confidence region of the random frequency response function for the total elastic energy of the structure: mean model prediction (thick solid line), mean response of the stochastic model (thick dashed line), confidence region (grey region)

Figure 9 displays the acoustic frequency response function for the internal acoustic pressure at a point located at the right passenger ear. It can be seen large fluctuations of the confidence region as function of the frequency. It can be concluded that the sensitivity of the acoustic pressure to random uncertainties depend on the frequency .

Finally, Figure 10 displays the total acoustic energy of the internal cavity and Figure 11 displays the total elastic energy of the structure. These two figures show that the confidence regions of the acoustic and elastic energies have a small sensitivity to random uncertainties. These conclusions concerning the global

quantities do not hold for local quantities. Since the structure is strongly heterogeneous, the sensitivity to random uncertainties depends on the local stiffness of the observed part of the structure. It seems that there is no so easy conclusion concerning the local response inside the acoustic cavity as a function of the frequency.

5 Conclusion

The confidence region of each random vibroacoustic frequency response function has been studied by using a non-parametric probabilistic model of random uncertainties in the structural stiffness matrix. The results obtained clearly show the role played by the random uncertainties on the vibration levels in the different structural parts and for the acoustic levels inside the cavity. The sensitivity of the flexible structural elements to random uncertainties is much more greater than for stiff structural elements.

References

[1] Germain, P (1973). *Cours de Mécanique des Milieux Continus*. Mason, Paris.
[2] Marsden, J.E, and Hugues, T. J. R. (1983). *Mathematical Foundations of Elasticity*. Prentice Hall, Englewood Cliffs, New Jersey.
[3] Ciarlet, P.G (1988). *Mathematical Elasticity, Vol.I: Three-dimensional Elasticity*. North Holland, Amsterdam.
[4] Ohayon, R., Soize, C. *Structural Acoustics And Vibration*, Academic Press.
[5] Landau, L. and Lifchitz, E. (1992b). *Fluid Mechanics*. Pergamon Press, Oxford.
[6] Lighthill, J. (1978). *Waves in Fluids*. Cambridge University Press, MA.
[7] Pierce, A. D. (1989). *Acoustics: An Introduction to its Physical Principles and Applications* . Acoust. Soc Am. Publications on Acoustics, Woodbury, NY, U.S.A. (originally published in 1981, McGraw-Hill, New York).
[8] Zienkiewicz, 0. C. and Taylor, R. L. (1989). *The Finite Element Method.* McGraw-Hill, New York , 4th edn. (vol. 1, 1989 and vol. 2, 1991).
[9] Lesueur, C. (1989). *Rayonnement Acoustique des Structures*. Eyrolles, Paris.
[10] Dautray, R. and Lions, J. L. (1992). *Mathematical Analysis And Numerical Methods for Science and Technology* . Springer-Verlag, Berlin.
[11] Meirovitch, L. (1990). *Dynamics and Control of Structures*. Wiley, New York.
[12] Argyris, J. and Mlejnek , H.P. (1991). *Dynamics of Structures*. North-Holland, Amsterdam.
[13] Bathe, K. J. and Wilson , E.L. (1976). *Numerical Methods in Finite Element Analysis*. Prentice-Hall, New York.
[14] Soize, C. (2000). *A Non-parametric Model of Random Uncertainties on Reduced Matrix Model in Structural Dynamics*, Probabilistic Engineering Mechanics, Vol. 15, No. 3, pp. 277-294.
[15] Soize, C. (2001). *Maximum entropy approach for modelling random uncertainties in transient elastodynamics*, J. Acoust. Soc. Amer., Vol. 109, No. 5, pp. 1979-1996.
[16] Soize, C. ,Random matrix theory for modelling uncertainties in computational mechanics, *Computer Methods in Applied Mechanics and Engineering*, (accepted for publication in March 2004).
[17] Serfling, R.J. (1980). *Approximation Theorems of Mathematical Statistics*, John Wiley & Sons.